

# A new universal law for the Liesegang pattern formation

Ferenc Izsák<sup>a)</sup>

Department of Applied Analysis, Eötvös University, P.O. Box 120, Budapest H-1518, Hungary

István Lagzi<sup>b)</sup>

Department of Physical Chemistry, Eötvös University, P.O. Box 32, Budapest H-1518, Hungary

(Received 16 December 2004; accepted 22 February 2005; published online 10 May 2005)

Classical regularities describing the Liesegang phenomenon have been observed and extensively studied in laboratory experiments for a long time. These have been verified in the last two decades, both theoretically and using simulations. However, they are only applicable if the observed system is driven by reaction and diffusion. We suggest here a new universal law, which is also valid in the case of various transport dynamics (purely diffusive, purely advective, and diffusion-advection cases). We state that  $p_{\text{tot}} \propto X_c$ , where  $p_{\text{tot}}$  yields the total amount of the precipitate and  $X_c$  is the center of gravity. Besides the theoretical derivation experimental and numerical evidence for the universal law is provided. In contrast to the classical regularities, the introduced quantities are continuous functions of time. © 2005 American Institute of Physics. [DOI: 10.1063/1.1893606]

## I. INTRODUCTION

A simple diffusion process coupled with nonlinear dynamics (arising from reactions) may produce various patterns. The first spatiotemporal pattern observed was the Liesegang phenomenon.<sup>1</sup> In this case, the quasiperiodic pattern occurs due to a precipitation reaction between a certain chemical reactant, which diffuses into a gel and another one, which is distributed in the gel. Recently, the trends of the investigation of the precipitation pattern formation are either to revisit and punctuate the existing empirical regularities,<sup>2-5</sup> or the observation and description of the pattern formation in more complex situations (redissolution of the precipitation zones due to complex formation producing moving patterns;<sup>6-8</sup> pattern formation in the case of various initial and boundary conditions<sup>9,10</sup>). Liesegang patterns are usually formed via interaction of inorganic compounds, therefore an interesting topic in recent studies is the coupling of the precipitation process and biological one.<sup>11,12</sup>

Detailed investigations on Liesegang phenomenon have shown four empirical regularities, in which the macroscopic quantities are connected with each other:  $x_n$ , the position of the  $n$ th precipitation zone measured from the junction point of electrolytes;  $w_n$ , the width of the  $n$ th band; and  $t_n$ , the time elapsed until its formation.

The spacing law states that the positions of the precipitate zones are members of a geometrical series:<sup>13</sup>

$$x_n = Q(1 + \hat{p})^n, \quad (1)$$

where  $1 + \hat{p}$  is the spacing coefficient and  $Q$  is the amplitude.

According to the time law of Liesegang patterning, the following relation holds:<sup>14</sup>

$$x_n \propto t_n^{1/2}. \quad (2)$$

The width law describes how the thickness of zones increases with their positions:<sup>15,16</sup>

$$w_n \propto x_n.$$

Experimental observations lead Matalon and Packter to the conclusion that  $\hat{p}$  is equal to the sum of some functions depending on the initial concentrations  $b_0$  of the inner and  $a_0$  of the outer electrolytes:<sup>17</sup>

$$p = F(b_0) + \frac{1}{a_0} G(b_0). \quad (3)$$

The above regularities are valid only if the transport of electrolytes is driven solely by diffusion. They have to be modified in the case of an imposed external field (e.g., electric field<sup>18-20</sup>). In the present study, we introduce a new universal law of Liesegang pattern formation, which is independent of the transport conditions (diffusive kinetics or an imposed migration of the species).

## II. MODELS

An *intermediate species* is introduced in the chemical mechanism to explain the precipitate formation.<sup>2,21</sup> This scheme contains two consecutive steps: initially the two reactants  $A$  (outer electrolyte) and  $B$  (inner electrolyte) react, and produce an intermediate species  $C$ , which is supposed to be in colloidal phase and may also diffuse. In the second step,  $C$  transforms into an insoluble precipitate  $P$ . The chemical mechanism described above is the following:



<sup>a)</sup>Also at Department of Applied Mathematics, University of Twente. Electronic mail: izsakf@cs.elte.hu

<sup>b)</sup>Electronic mail: lagzi@vuk.chem.elte.hu

## A. Theoretical

First, we summarize all necessary simplified assumptions to derive our new law: (i) The investigated system is *one* dimensional. Recently, experimental and numerical studies have shown that the most general law (time law) has a weak distortion compared to the effect of the planar diffusion front propagation. This has been observed in the case of circular experimental setup in two dimension (2D) and 3D (Ref. 22) (called curvature effect in the literature<sup>23</sup>). (ii) We neglect the effect of background ions (which do not turn into precipitate in the given system): we assume that they do not play an important role in the evolution of the patterns in the absence of an electric field.<sup>24</sup> (iii) Density of the intermediate species  $c_0$  is constant behind the reaction front.<sup>25</sup> (iv)  $C$  is segregated into high density zones (precipitation bands with concentration  $c_h$ ) and into low density zones (gaps between the precipitation bands with concentration  $c_l$ ).<sup>25</sup> (v) Species  $C$  fulfills the mass conservation law. (vi) The width of the bands  $w_n$  is negligible compared to the given band position, i.e.,  $w_n \ll x_n$ . (vii) The concentration  $c_l$  of the precipitate between the bands is negligible compared to  $c_h$  and  $c_0$ , i.e.,  $c_0, c_h \gg c_l$ . (viii)  $c_0$  is linearly proportional to the initial concentration of the inner electrolyte,<sup>3</sup> i.e.,  $c_0 \propto b_0$ . Using the mass conservation law (v) together with (iii) and (iv), we obtain the following relation:

$$(x_{n+1} - x_n)c_0 = (x_{n+1} - x_n - w_n)c_l + w_nc_h$$

and therefore,

$$(x_{n+1} - x_n)(c_0 - c_l) = w_n(c_h - c_l).$$

Applying the spacing law (1), we can rewrite the equation above as

$$w_n = \frac{\hat{p}(c_0 - c_l)}{c_h - c_l} x_n =: \zeta x_n. \quad (6)$$

This relation is a so-called width law.<sup>5,25</sup> Next, the total amount of the precipitate  $p_{\text{tot}}$  and the center of gravity of the precipitation band system  $X_c$  are defined as

$$p_{\text{tot}}(t) = \sum_{n=1}^N p_n(t), \quad X_c(t) = \frac{\sum_{n=1}^N p_n(t)x_n}{p_{\text{tot}}(t)}, \quad (7)$$

where  $p_n$  is the amount of the precipitate at  $x_n$  and  $N$  is the total number of bands at  $t$ . It should be noted that  $N$  depends on time  $t$  and it is an increasing function. Quantities  $p_{\text{tot}}$  and  $X_c$  introduced here play a central role in our analysis. Since  $p_n = w_nc_h$ , we can rewrite (7):

$$p_{\text{tot}}(t) = \sum_{n=1}^N w_nc_h, \quad X_c(t) = \frac{\sum_{n=1}^N w_nc_h x_n}{\sum_{n=1}^N w_nc_h},$$

and applying the width law (6) we obtain

$$p_{\text{tot}}(t) = \zeta c_h \sum_{n=1}^N x_n, \quad X_c(t) = \frac{\zeta c_h \sum_{n=1}^N x_n^2}{\zeta c_h \sum_{n=1}^N x_n}.$$

Using the spacing law (1) we get the limit

$$\frac{\sum_{n=1}^N x_n \sum_{n=1}^N x_n}{\sum_{n=1}^N x_n^2} \rightarrow \frac{\hat{p} + 2}{\hat{p}} \quad \text{if } N \rightarrow \infty,$$

in this way for  $N$  big enough we may use the relation

$$\frac{p_{\text{tot}}(t)}{X_c(t)} = \zeta c_h \frac{\hat{p} + 2}{\hat{p}},$$

where

$$\zeta = \frac{\hat{p}(c_0 - c_l)}{c_h - c_l}.$$

It makes sense to use this approximation, since  $N \rightarrow \infty$  as  $t \rightarrow \infty$  and we are interested in the long time behavior of the system. Application of the last two assumptions (vii–viii) leads us to the equality

$$\frac{p_{\text{tot}}(t)}{X_c(t)} = b_0(\hat{p} + 2). \quad (8)$$

From the experimental point of view, it is not easy to measure  $c_0$ ,  $c_l$ , and  $c_h$ , therefore it is useful to eliminate these quantities, which is accomplished in Eq. (8) depending only on well-measurable quantities.

Finally, substituting the Matalon–Packter law (3) into Eq. (8) a more general form is obtained:

$$\frac{p_{\text{tot}}(t)}{X_c(t)} = b_0(F(b_0) + 2) + \frac{b_0}{a_0}G(b_0). \quad (9)$$

In this way we conclude that the total amount of the precipitate is linearly proportional to the center of gravity of the precipitation band system ( $p_{\text{tot}} \propto X_c$ ). Note that  $F$  and  $G$  are fixed during the individual experiments. An interesting consequence of Eq. (9) is that one experiment can validate the linear dependence. We also point out the favorable property of  $p_{\text{tot}}$  and  $X_c$ : they depend continuously on time.

## B. Numerical

We would like to prove the universality of our new relation  $p_{\text{tot}}/X_c \propto \text{const}$ , i.e., this one does not depend on the transport condition of the invading electrolyte. Therefore, we allow also advection for the outer electrolyte  $A$  (besides the existing diffusion process). We will investigate the pattern formation phenomenon in the case of purely diffusive, purely advective, and mixed (diffusion-advection) conditions. For the sake of simplicity, a constant and uniform advection field was applied.

The governing equations of such pattern formation in 1D corresponding to the scheme (4) and (5) are the following:

$$\frac{\partial a}{\partial \tau} = D_a \frac{\partial^2 a}{\partial x^2} - u \frac{\partial a}{\partial x} - kab, \quad (10a)$$

$$\frac{\partial b}{\partial \tau} = D_b \frac{\partial^2 b}{\partial x^2} - kab, \quad (10b)$$

$$\frac{\partial c}{\partial \tau} = D_c \frac{\partial^2 c}{\partial x^2} + kab - \kappa_1 \Theta(c - c^*)c - \kappa_2 cp, \quad (10c)$$

$$\frac{\partial p}{\partial \tau} = \kappa_1 \Theta(c - c^*)c + \kappa_2 cp, \quad (10d)$$

where all quantities are dimensionless.  $a$ ,  $b$ , and  $c$  yield the concentrations of  $A$ ,  $B$ , and  $C$ , respectively, while  $p$  yields the amount of the precipitate.  $D_a$ ,  $D_b$ , and  $D_c$  are the diffusion coefficients of the corresponding species, while  $u$  yields the advection field velocity.  $k$  is the chemical rate constant for Eq. (4), and  $\kappa_1$ ,  $\kappa_2$  are the rate constants for the nucleation and the autocatalytic precipitate formation (5), respectively. The two terms in (10d) correspond to homogeneous nucleation after that an autocatalytic precipitate growth occurs.  $\Theta$  is the Heaviside step function. The main idea of *nucleation and precipitate growth* model is that *nucleation* occurs when the local concentration  $c$  of the intermediate species reaches the nucleation threshold  $c^*$ . At the same time  $c \rightarrow 0$  (since  $C$  transforms into precipitate), whenever some precipitate already exists (due to the autocatalytic process).

The partial differential equations were solved using a “method of lines” technics. Spatially a finite difference discretization on a 1D equidistant grid was applied. The time integration has been executed using a second-order Runge–Kutta method to solve the produced ordinary differential equations. During the simulation (10a)–(10d) were equipped with the following initial and boundary conditions:

$$a(0,x) = a_0 \Theta(-x), \quad b(0,x) = b_0 \Theta(x),$$

$$c(0,x) = p(0,x) = 0,$$

$$a|_{x=0} = a_0,$$

$$\left. \frac{\partial b}{\partial x} \right|_{x=0} = \left. \frac{\partial c}{\partial x} \right|_{x=0} = \left. \frac{\partial a}{\partial x} \right|_{x=l} = \left. \frac{\partial b}{\partial x} \right|_{x=l} = \left. \frac{\partial c}{\partial x} \right|_{x=l} = 0,$$

where  $l$  is the length of the diffusion column. In all simulations the parameter set  $D_a = D_b = 1.0$ ,  $D_c = 0.1$ ,  $k = 1.0$ ,  $\kappa_1 = 1.0$ ,  $\kappa_2 = 10^2$ ,  $c^* = 0.1$ , and  $l = 480$  was used, while  $a_0$  and  $b_0$  were varied. The grid spacing was  $\Delta x = 0.4$ , and the numerical simulations were performed with the time step  $\Delta \tau = 0.001$ .

### III. EXPERIMENT

A solution of  $K_2Cr_2O_7$  (Reanal, 0.0036M) and gelatine (Reanal) was heated to 80 °C and stricted continuously to complete dissolution of the gelatine. The solution was poured into a  $U$  tube (of diameter 0.5 cm and length 25 cm) and was allowed to cool to room temperature (23 °C  $\pm$  1 °C).

After 24 h, the gel was contacted with the solution of  $K_2Cr_2O_7$  (0.0036M) and  $AgNO_3$  (5 m/m %), respectively.

Temporal evolution of the Liesegang patterns was monitored by a computer controlled image capturing system using reflected light from a halogen lamp. The average “build up” time of the individual bands is about 1 h: images were collected in every 25 min. During the gray scale analysis of the pictures it was supposed that the amount of the precipitate is proportional to the peak area of the intensity of the scattered light. The total amount of the precipitate and the center of gravity were determined using the observation along a certain line, and the calculations were based on Eq. (7). The image sequence in this procedure was generated by ORIGIN data graphing and analysis software.

### IV. RESULTS AND DISCUSSIONS

At first, we focused on the experimental evidence of the new relation described in the theoretical part. Figure 1 shows the evolution of the total amount of the precipitate [Fig. 1(a)] and the center of gravity of the precipitate [Fig. 1(b)] in the diffusion column (gel medium), respectively: these quantities depend linearly on the square root of time. We also depicted the final precipitation pattern structure and the relation between  $p_{tot}$  and  $X_c$  [Fig. 1(c)], which is also linear piecewise: we distinguished two regimes. In many experiments one can observe initially a continuous precipitate zone initiated from the junction point of the electrolytes up to a certain position  $x_*$  (transition point), afterwards the evolution of well separated precipitation bands occurs. In lack of pattern formation phenomena homogeneous distribution of precipitate can be assumed within this zone which gives that the total amount of the precipitate ( $p_{tot}$ ) is linearly proportional to  $x_*$ . For the same reason,  $X_c \sim x_*$  also holds and therefore,  $p_{tot} \sim X_c$  in this case. At the same time, the coefficient of the proportionality can be different from that obtained after the transition point, as shown in [Fig. 1(a) and 1(c)].

As known for a long time,<sup>14</sup> the (discrete) band position  $x_n$  measured from the junction point of the electrolytes depends linearly on the square root of its formation time. Usually, in the experiments the junction point is the gel surface, which initially separates the electrolytes. This relation is the well-known time law (2), which is an immediate consequence of the diffusive behavior of the invading electrolyte. Since the center of gravity is originated from  $x_n$ , it is not surprising that  $X_c$  has a similar linear evolution trend. The above mentioned two continuous variables ( $p_{tot}, X_c$ ) have linear dependence on the square root of time, therefore they will be linearly proportional to each other, i.e.,  $p_{tot} \propto X_c$ , as has been predicted theoretically in both regimes.

We also confirmed our experimental and theoretical findings using numerical simulations. Moreover, we can get some new predictions on the behavior of the system. As a usual approach we applied nucleation and growth mechanism to describe the precipitation pattern formation. In a former study, Antal *et al.* investigated the origin of the Matalon–Packter law and proposed different forms in special cases (depending on the applied precipitation mechanism).

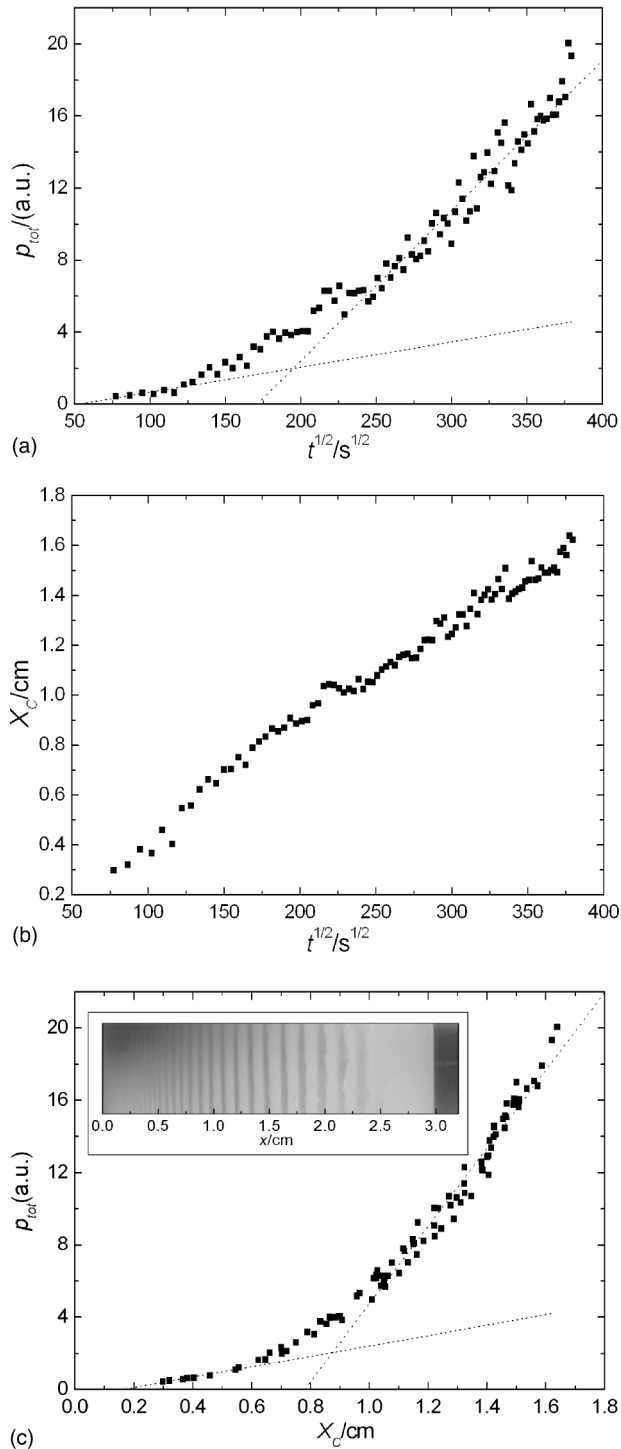


FIG. 1. Results of laboratory experiments: (a) dependence of the total amount of the precipitate ( $p_{\text{tot}}$ ) and (b) the center of gravity of the precipitate ( $X_c$ ) on the square root of the elapsed time; (c) pattern structure and dependence of  $p_{\text{tot}}$  on  $X_c$ .

For our case (nucleation and growth) they found that  $F(b_0) \propto 1/b_0$  and  $G(b_0) \propto \text{const.}$  Using these we can rewrite the general form (9) into

$$p_{\text{tot}} \propto b_0 \left( 2 + \frac{G^*}{a_0} \right) X_c, \quad (11)$$

where  $G^*$  is a constant obtained from the function  $G(b_0)$ .

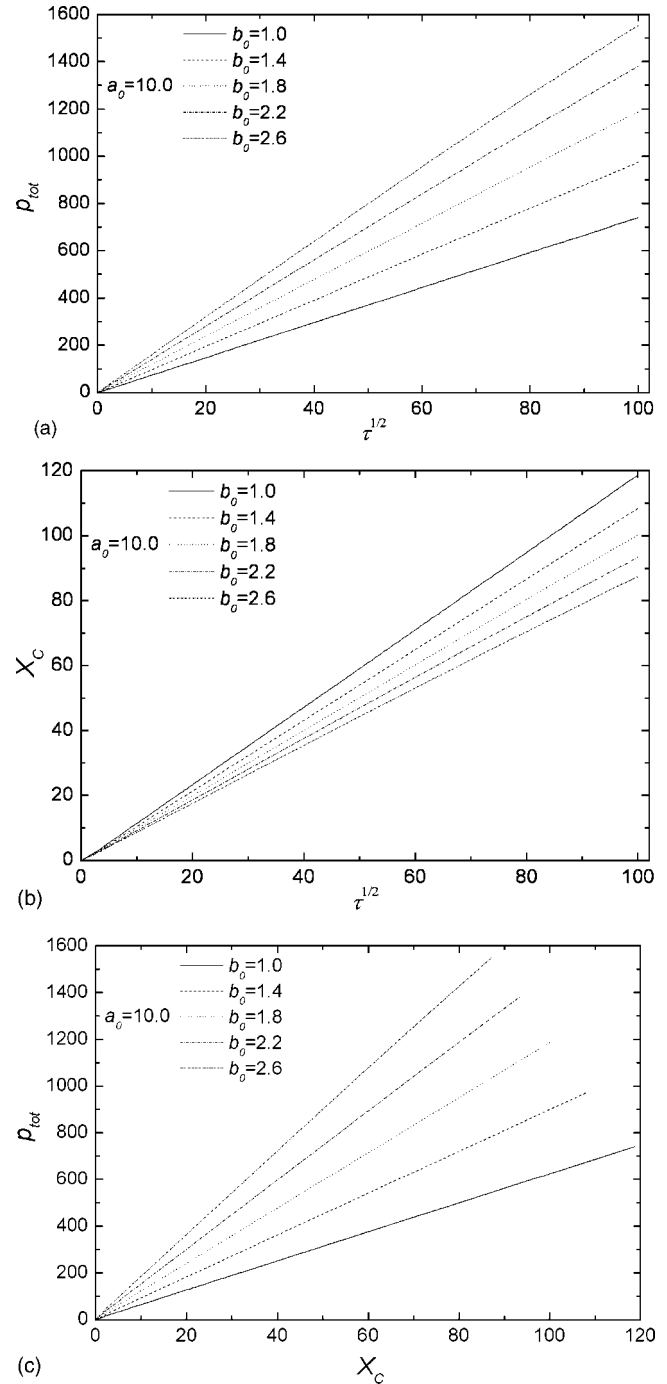


FIG. 2. Results of the numerical simulations fixing the concentration of the outer electrolyte in case of purely diffusive dynamics: (a) dependence of the total amount of the precipitate ( $p_{\text{tot}}$ ) and (b) the center of gravity of the precipitate ( $X_c$ ) on the square root of the elapsed time; (c) dependence of  $p_{\text{tot}}$  on  $X_c$ .

We investigated the evolution of the patterns by fixing the concentration of one electrolyte and varying that of the other one. Figure 2 presents the variation of  $p_{\text{tot}}$  and  $X_c$  (as in experiments) at fixed values of the outer electrolyte concentration. The linear dependence between these quantities can be clearly seen. There is a good accordance with the theoretical and experimental observations. Increasing the concentration of the inner electrolyte ( $b_0$ ) the slope of the  $p_{\text{tot}}-X_c$  linear curves is also increased. The fact that  $a_0$  is fixed implies that  $2 + G^*/a_0$  is constant, therefore  $p_{\text{tot}} \propto b_0 X_c$  (the slope is lin-

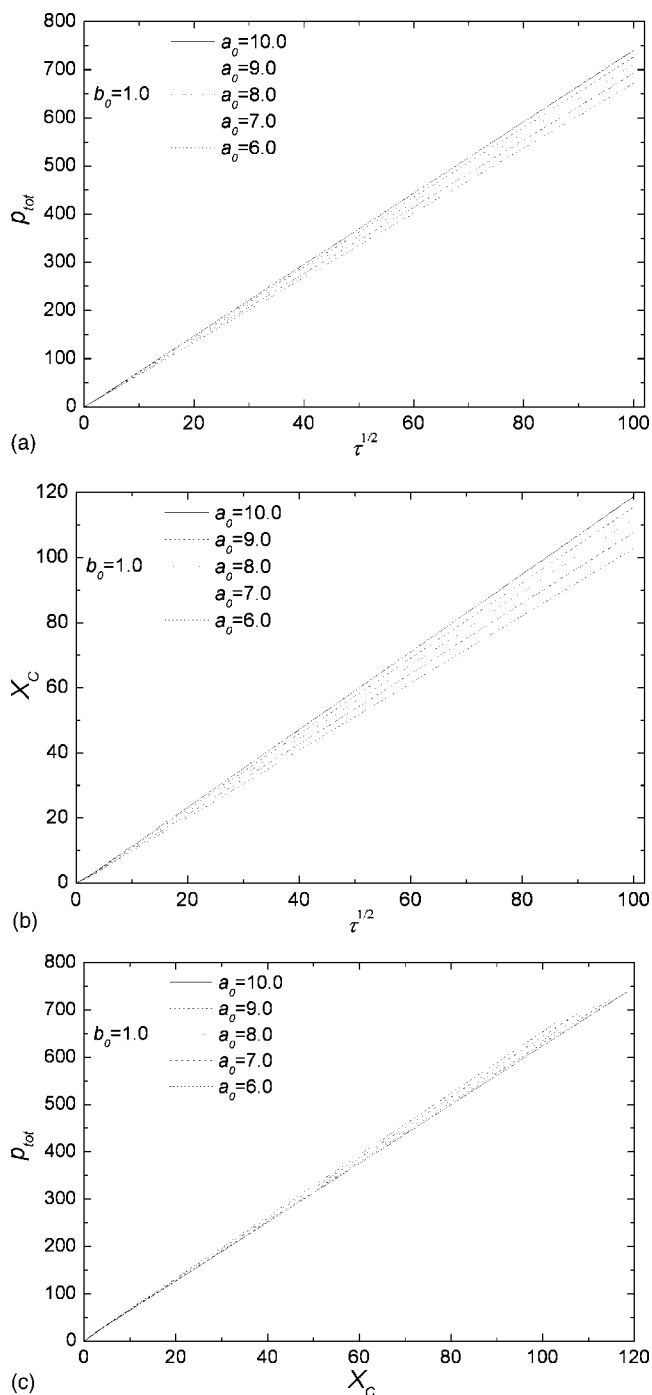


FIG. 3. Results of the numerical simulations fixing the concentration of the inner electrolyte in case of purely diffusive dynamics: (a) dependence of the total amount of the precipitate ( $p_{\text{tot}}$ ) and (b) the center of gravity of the precipitate ( $X_C$ ) on the square root of the elapsed time; (c) dependence of  $p_{\text{tot}}$  on  $X_C$ .

early proportional to  $b_0$ ). In the reverse case fixing the concentration of the inner electrolyte ( $b_0$ ) and varying that of the outer one, an opposite trend was observed: the slope of the  $p_{\text{tot}}-X_C$  linear curves decreases as  $a_0$  is increased (Fig. 3). This finding can be explained by taking  $b_0$  fixed in Eq. (11): in this case  $p_{\text{tot}} \propto (1/a_0)X_C$  (the slope is linearly proportional to  $1/a_0$ ). Equation (11) can be rewritten as

$$\frac{p_{\text{tot}}}{X_C} \propto b_0 \left( 2 + \frac{G^*}{a_0} \right).$$

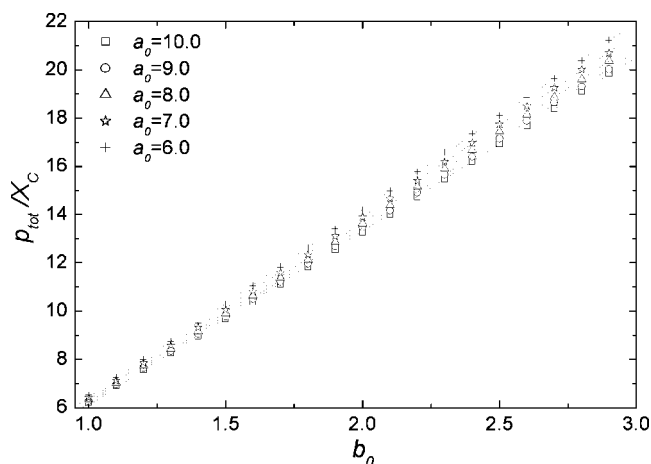


FIG. 4.  $p_{\text{tot}}/X_C$  as a function of the initial concentration of the inner electrolyte ( $b_0$ ) at different constant outer electrolyte concentrations ( $a_0$ ).

The plot of  $p_{\text{tot}}/X_C$  vs  $b_0$  in the individual runs indicated two new observations: first, the existing dependence between  $p_{\text{tot}}/X_C$  and  $b_0$  is linear (at fixed  $a_0$ ); second, the slopes of the linear curves are linearly proportional to  $1/a_0$ . These two theoretical predictions are in a good agreement with the results of the detailed numerical experiments as shown in Fig. 4.

In Fig. 5 we depicted the spatial distribution of the intermediate species  $C$  and the precipitate  $P$ . Initially, a continuous precipitation zone could be observed as in the experiments. However, we did not obtain well detectable linear regime corresponding to the continuous precipitate formation since this region was relatively thin.

We compared the time dependence of  $p_{\text{tot}}$  and  $X_C$  in case of purely diffusive kinetics, in case of purely advective kinetics, and in the mixed case. In this way we point out the universality of our new law  $p_{\text{tot}} \propto X_C$ : this relation always holds; at the same time, the ratio of these quantities depends on the transport conditions. Figure 6 illustrates the time dependence of  $p_{\text{tot}}$  and  $X_C$ , and the relation between them. In

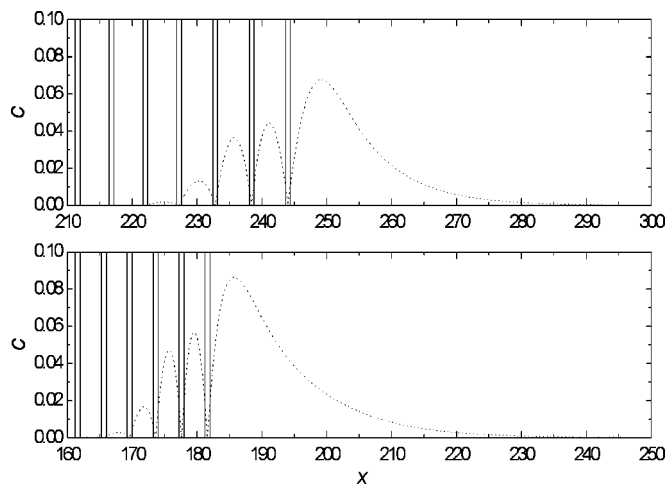


FIG. 5. Spatial distribution of the intermediate species  $C$  and precipitate  $P$  for two different initial concentration sets of the outer ( $a_0$ ) and inner ( $b_0$ ) electrolyte at  $\tau=10\,000$ , respectively (top— $a_0=10.0$ ,  $b_0=1.0$ ; bottom— $a_0=10.0$ ,  $b_0=2.6$ ). The dotted and solid lines represent the concentration  $c$  profiles of  $C$  and  $P$ .

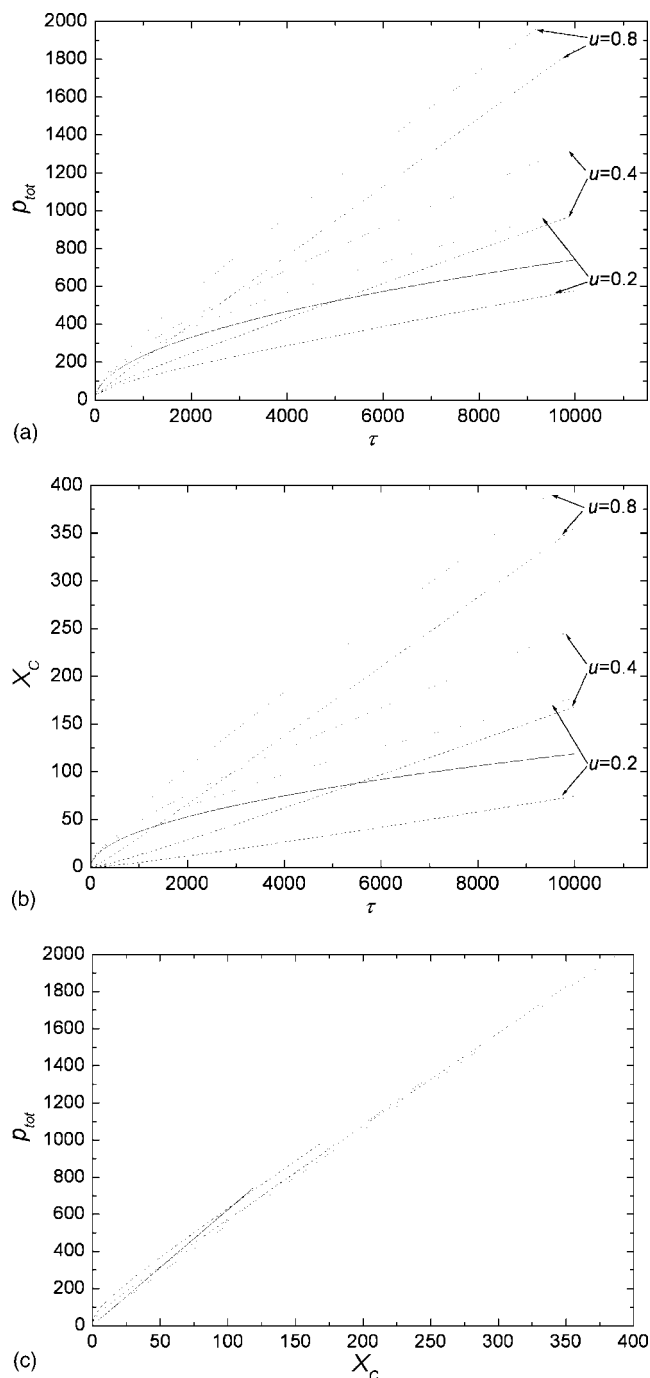


FIG. 6. Results of the numerical simulations in case of purely diffusive dynamics (solid line)— $D_a \neq 0, u=0$ ; in case of purely advective dynamics (dashed line)— $D_a=0, u \neq 0$ ; and in diffusion-advection case (dotted line)— $D_a \neq 0, u \neq 0$ , where  $u$  is the advection field velocity and  $D_a$  is the diffusion coefficient of the A species. (a) Dependence of the total amount of the precipitate ( $p_{\text{tot}}$ ) and (b) the center of gravity of the precipitate ( $X_c$ ) on the square root of the elapsed time; (c) dependence of  $p_{\text{tot}}$  on  $X_c$ . In Fig. 5(c) the long and short dashed lines correspond to  $u=0.8$  and  $u=0.4$ , respectively. The same applies for the dotted lines. We used the initial concentrations:  $a_0=10.0$ ,  $b_0=1.0$ .

the diffusion-advection process one can observe that initially the system is driven by diffusion: the flux is generated mostly due to the high concentration gradient of the invading electrolyte. Later on, since this gradient essentially decreases, the advective flux will dominate. After a certain period, the evolution will be linear in time as shown in Figs.

6(a) and 6(b), respectively. Assuming advective dynamics only the evolution of  $p_{\text{tot}}$  and  $X_c$  is also linear. At long enough times (depending on the advection field velocity) the quantities above overtake that of in purely diffusive situation. One can observe that the velocity of the motion of  $p_{\text{tot}}$  and  $X_c$  depends on the advection velocity only, if this exists (the curves corresponding to the same advection velocity will be parallel after some time). Note that in the purely diffusive case these variables depend linearly on the square root of time. If the transport of the outer electrolyte is generated by a constant drift<sup>26</sup> (caused either by advection or autocatalytic chemical front propagation<sup>27</sup>), it results in an equidistant pattern structure with bands of constant thickness. The coupling of fluid flow and precipitation process have a great relevance to explain several structures in geoscience.<sup>28–31</sup> It should be mentioned that the effect of diffusion cannot be neglected in laboratory experiments, consequently, the purely advective dynamics is only a theoretical assumption. It is also clear that advection influences the motion of all species, but owing to the high concentration differences between, it can be assumed that the pattern formation dynamics is essentially determined by the flux of the highest concentration species (this is the invading electrolyte in the Liesegang systems). The advection terms of the species B and C omitted in our governing Eqs. (10b) and (10c) may play an essential role in geological applications. The applicability of the proposed relation needs also to estimate the Péclet numbers (in case of convection regime), which can be the basis of a further detailed analysis.

## V. CONCLUSIONS

We suggested a new universal law for a class of Liesegang pattern formation phenomena concerning the time dependent quantities of the precipitate:  $p_{\text{tot}}$ , the total amount of precipitate and  $X_c$ , the position (measured from the junction point of electrolytes) of the center of gravity of precipitate. An explicit form for  $p_{\text{tot}}/X_c$  has been derived assuming diffusive dynamics only, which was confirmed by our real experiments. Moreover, using numerical simulations, we pointed out that the same connection is valid by changing the transport conditions of the invading electrolyte: we have stated that  $p_{\text{tot}} \propto X_c$  and this relation holds under various circumstances (diffusive, advective, and diffusive-advective dynamics) in contrast to the classical laws proposed earlier.

## ACKNOWLEDGMENTS

The authors are very grateful to Professor Zoltán Rácz and Judit Zádor for helpful discussions. They also acknowledge the support of the Hungarian OTKA Postdoctoral Fellowship (OTKA Grant No. D048673) and the Hungarian Ministry of Education (OMFB Grant No. 00585/2003IKTA5-137).

<sup>1</sup>R. E. Liesegang, Naturwiss. Wochenschr. **11**, 353 (1896).

<sup>2</sup>M. Droz, J. Magnin, and M. Zrinyi, J. Chem. Phys. **110**, 9618 (1999).

<sup>3</sup>T. Antal, M. Droz, J. Magnin, Z. Rácz, and M. Zrinyi, J. Chem. Phys. **109**, 9479 (1998).

<sup>4</sup>J. George and G. Varghese, Chem. Phys. Lett. **362**, 8 (2002).

<sup>5</sup>J. George and G. Varghese, J. Colloid Interface Sci. **282**, 397 (2005).

- <sup>6</sup>M. Zrínyi, L. Gálfi, É. Smidróczki, Z. Rácz, and F. Horkay, *J. Phys. Chem.* **95**, 1618 (1991).
- <sup>7</sup>R. Sultan and S. Sadek, *J. Phys. Chem.* **100**, 16912 (1996).
- <sup>8</sup>I. Lagzi, *J. Phys. Chem. B* **107**, 13750 (2003).
- <sup>9</sup>P. Hantz, *J. Phys. Chem. B* **104**, 4266 (2000).
- <sup>10</sup>S. C. Müller and J. Ross, *J. Phys. Chem. A* **107**, 7997 (2003).
- <sup>11</sup>V. V. Kravchenko, A. B. Medvinskii, V. I. Emelyanenko, A. N. Reshetilov, and G. R. Ivanitskii, *Biofizika* **45**, 93 (2000).
- <sup>12</sup>A. B. Medvinskii, A. V. Rusakov, M. A. Tsyganov, and V. V. Kravchenko, *Biofizika* **45**, 525 (2000).
- <sup>13</sup>K. Jablczyński, *Bull. Soc. Chim. Fr.* **33**, 1592 (1923).
- <sup>14</sup>H. W. Morse and G. W. Pierce, *Proc. Am. Acad. Arts Sci.* **38**, 625 (1903).
- <sup>15</sup>K. M. Pillai, V. K. Vaidyan, and M. A. Ittyachan, *Colloid Polym. Sci.* **258**, 831 (1980).
- <sup>16</sup>S. C. Müller, S. Kai, and J. Ross, *J. Phys. Chem.* **86**, 4078 (1982).
- <sup>17</sup>R. Matalon and A. Packter, *J. Colloid Sci.* **10**, 46 (1955).
- <sup>18</sup>I. Lagzi, *Phys. Chem. Chem. Phys.* **4**, 1268 (2002).
- <sup>19</sup>R. F. Sultan, *Phys. Chem. Chem. Phys.* **4**, 1253 (2002).
- <sup>20</sup>I. Lagzi and F. Izsák, *Phys. Chem. Chem. Phys.* **5**, 4144 (2003).
- <sup>21</sup>J. B. Keller and S. I. Rubinow, *J. Chem. Phys.* **74**, 5000 (1981).
- <sup>22</sup>I. Lagzi, A. Volford, and A. Büki, *Chem. Phys. Lett.* **396**, 97 (2004).
- <sup>23</sup>J. J. Tyson and J. P. Keener, *Physica D* **32**, 327 (1988).
- <sup>24</sup>T. Unger and Z. Rácz, *Phys. Rev. E* **61**, 3583 (2000).
- <sup>25</sup>Z. Rácz, *Physica A* **274**, 50 (1999).
- <sup>26</sup>M. I. Lebedeva, D. G. Vlachos, and M. Tsapatsis, *Phys. Rev. Lett.* **92**, 088301 (2004).
- <sup>27</sup>I. Lagzi and D. Kármán, *Chem. Phys. Lett.* **372**, 831 (2003).
- <sup>28</sup>P. Ortoleva, E. Merino, C. Moore, and J. Chadam, *Am. J. Sci.* **287**, 979 (1987).
- <sup>29</sup>E. F. McBride, A. Abdel-Wahab, and A. R. M. El-Younsy, *Sedimentology* **46**, 733 (1999).
- <sup>30</sup>F. Marko, D. Pivko, and V. Hurai, *Geol. J.* **47**, 241 (2003).
- <sup>31</sup>C. L. Ciobanu and N. J. Cook, *Ore Geol. Rev.* **24**, 315 (2004).